Avalanches in the raise and peel model in the presence of a wall

2013 J. Phys. A: Math. Theor. 46 265001

(http://iopscience.iop.org/1751-8121/46/26/265001)

J. Phys. A: Math. Theor. **46** (2013) 265001 (15pp) doi:10.1088/1751-8113/46/26/265001

Avalanches in the raise and peel model in the presence of a wall

Edwin Antillon[1], **Birgit Wehefritz-Kaufmann**[1,2] **and Sabre Kais**[1,3,4]

[1] Department of Physics, Purdue University, West Lafayette, IN 47907, USA
[2] Department of Mathematics, Purdue University, West Lafayette, IN 47907, USA
[3] Department of Chemistry, Purdue University, West Lafayette, IN 47907, USA
[4] Qatar Environment and Energy Research Institute, Doha, Qatar

E-mail: ebkaufma@math.purdue.edu

Received 18 December 2012, in final form 17 April 2013
Published 6 June 2013
Online at stacks.iop.org/JPhysA/46/265001

Abstract
We investigate a non-equilibrium one-dimensional model known as the raise and peel model describing a growing surface which grows locally and has non-local desorption. For specific values of adsorption (u_a) and desorption (u_d) rates, the model shows interesting features. At $u_a = u_d$, the model is described by a conformal field theory (with conformal charge $c = 0$) and its stationary probability can be mapped onto the ground state of the XXZ quantum chain. Moreover, for the regime $u_a \geqslant u_d$, the model shows a phase in which the avalanche distribution is scale-invariant. In this work, we study the surface dynamics by looking at avalanche distributions using a finite-sized scaling formalism and explore the effect of adding a wall to the model. The model shows the same universality for the cases with and without a wall for an odd number of tiles removed, but we find a new exponent in the presence of a wall for an even number of tiles released in an avalanche. New insights into the effect of parity on avalanche distributions are discussed and we provide a new conjecture for the probability distribution of avalanches with a wall obtained by using an exact diagonalization of small lattices and Monte Carlo simulations.

PACS numbers: 05.10.Ln, 05.70.Jk, 05.40.−a

(Some figures may appear in colour only in the online journal)

1. Introduction

The raise and peel model (RPM) is a Markov process first proposed in [1] describing the evolution of a growing surface as a fluctuating interface in one dimension. This model has been found to belong to a new universality class in non-equilibrium phenomena [1–5]. For a particular value of the adsorption (u_a) and desorption (u_d) rates, the model exhibits the phenomenon of self-organized criticality [6, 7] where probability distributions of desorption events show long tails and are characterized by a varying critical exponent that depends on a single parameter given by the ratio of the adsorption and desorption rates [4, 5].

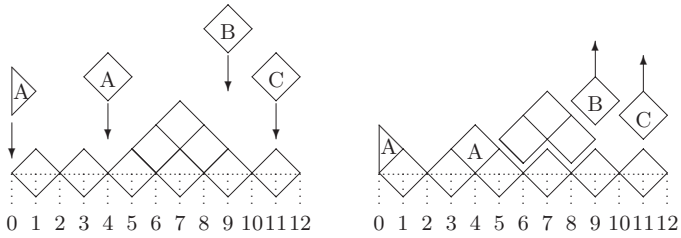

Figure 1. Three possible cases shown for a lattice with $L = 12$ sites. (*A*) A tile attaches to the surface in the bulk or a half-tile attaches to site 0. (*B*) A tile removes a layer. (*C*) A tile is reflected. The *substrate*, denoted by the bottom tiles touching the dashed lines, remains fixed at all times.

When adsorption and desorption rates are equal, the model becomes solvable. This goes back to a connection established by Razumov and Stroganov [8–10] which relates the two-dimensional dense $O(n = 1)$ fully packed loop models (enumerating the stationary state probability distributions of RPM) to the ground-state wavefunctions of the XXZ chain [5, 11, 12] which in turn can be related to the stationary states of the RPM. Moreover, at this point, the spectra can be described by a conformal field theory with the central charge $c = 0$ [13, 14]. This offers a nice mathematical structure, which allows us to make conjectures using small lattices for expressions of physical quantities that remain valid for any system size.

In this work, we study the effect that a wall on one side of the system has on the avalanche distribution. We will abbreviate the raise and peel model in the presence of a wall by RPMW. So far, little is known about this model which is obtained from the RPM when the boundary is allowed to fluctuate. In this work, we focus on an even number of sites: $L = 2n$ ($n \in \mathbb{Z}$). Some other interesting results for the model with a wall have been reported, for example, in [15, 16]. In section 2, we describe the stochastic rules for the model with and without a wall and highlight some of the known results for these two cases. In section 3, we discuss the energy spectra of the stochastic Hamiltonian of the XXZ quantum chain which describe the RPM and the RPMW models for $u = 1$. Finally in section 4, we compute critical exponents for avalanche distributions in the RPM and the RPMW and derive new conjectures for probability distributions with a wall.

2. Raise and peel models

The RPM describes a growing and fluctuating interface. It is defined as follows: we consider a one-dimensional lattice with $L+1$ sites and open boundary conditions. An interface is formed by attaching at each site non-negative integer heights h_i which obey the restricted-solid-on-solid rules

$$h_{i+1} - h_i = \pm 1; \quad i = 0, 1, \ldots, L. \tag{1}$$

The initial configuration is the bare substrate (see figure 1) with all $h_i = 0$; $i = 0, 1, \ldots, L$. Tiles from rarefied gas are dropped onto this surface with a certain probability. For the RPM, a tile from the gas hits the site i with probability $P_i = \frac{1}{L-1}$ for $0 < i < L$. Nothing happens on the two boundary sites $i = 0$ and $i = L$.

For the RPMW, the site $i = 0$ becomes active and the probabilities are changed as follows: the probability of landing on a given site (P_i) in the bulk ($0 < i < L$) is given by a uniform distribution $P_i = \frac{1}{L+b-1}$ that depends on an additional parameter b which is the boundary rate (the bulk rate being equal to 1). With probability $P_0 = \frac{b}{L+b-1}$, a half-tile hits site 0. The rightmost site ($i = L$) is still never hit by a tile; thus, the probability is $P_L = 0$.

Depending on the value of the slope at site i, $s_i = (h_{i+1} - h_{i-1})/2$, the following processes can occur:

- Case A: $s_i = 0$ *and* $h_i < h_{i-1}$. *Tile lands on a local minimum*
  For sites $i > 0$, a tile attaches to the substrate at site i with rate u_a. If a tile is attached to site i, the height on that site changes by 2: $h_i \to h_i + 2$.
- Case B: $s_i = 1$ *or* $s_i = -1$. *Tile lands on a non-zero slope*
  For $s_i = 1$; $i = 1, \ldots, L-1$: with rate u_d, the tile is reflected after triggering the desorption of a layer of tiles from the segment $(h_j > h_i = h_{i+k},\ j = i+1, \ldots, i+k-1)$, thus changing all the heights $h_j \to h_j - 2$ for $j = i+1, \ldots, i+k-1$. If $s_0 = h_1 = h_0 = 1$, the half-tile gets absorbed with rate b and the height on that site changes by 2: $h_0 \to h_0 + 2$.
  For $s_i = -1$: with rate u_d, the tile is reflected after triggering the desorption of a layer of tiles from the segment $(h_j > h_i = h_{i-k},\ j = i-k+1, \ldots, i-1)$, thus changing all the heights $h_j \to h_j - 2$ for $j = i-k+1, \ldots, i-1$. If $s_0 = h_1 = h_0 = -1$, the half-tile is reflected. Thus, the left boundary is the only site with a local absorption/reflection.
- Case C: $s_i = 0$ *and* $h_i > h_{i-1}$. *Tile lands on a local maximum*
  The tile is reflected and nothing happens.

This stochastic process in continuum time can be described by the *master equation* [17, 18]:

$$\frac{\mathrm{d}}{\mathrm{d}t} P_\alpha(t) = -\sum_\beta H_{\alpha,\beta} P_\beta(t) \tag{2}$$

where $P_\alpha(t)$ is the (unnormalized) probability of finding the system in one of the states $|\alpha\rangle$ at time t, and $H_{\alpha,\beta}$ is the rate for the transition $|\alpha\rangle \to |\beta\rangle$. Since this is an intensity matrix, there is at least one zero eigenvalue [4] and its corresponding eigenvector $|0\rangle$ gives the probabilities in the *stationary* state

$$\langle 0|H = 0, \quad \langle 0| = (1, 1, \ldots, 1) \tag{3}$$

$$H|0\rangle = 0, \quad |0\rangle = \sum_\alpha P_\alpha |\alpha\rangle, \quad P_\alpha = \lim_{t\to\infty} P_\alpha(t). \tag{4}$$

For the special case in which the rates are equal $u_a = u_d$, the Hamiltonian can be written in terms of the Temperley–Lieb algebra defined in terms of generators $e_1, e_2, \ldots, e_L$ satisfying the following commutation relations [19]:

$$\begin{aligned} &e_i^2 = e_i \\ &e_i e_{i+1} e_i = e_i \\ &e_i e_{i-1} e_i = e_i \\ &[e_i, e_j] = 0 \quad \text{for } |i-j| \geqslant 2, \end{aligned} \tag{5}$$

while the one-boundary term e_0 at site $i = 0$ satisfies the following constraint [20, 21]:

$$e_0^2 = e_0, \quad e_1 e_0 e_1 = e_1, \quad e_0 e_i = e_i e_0 \quad \text{if } i > 1. \tag{6}$$

The algebra given by the generators e_i; $i = 0, \ldots, L$ is the one-boundary Temperley–Lieb algebra proposed in [22] as the 'blob algebra' which was subsequently studied by many other authors; see, e.g., [23, 20]. The generators e_i have the following representation in terms of Pauli spin matrices:

$$e_i = \tfrac{1}{2}\left\{\sigma_i^x \sigma_{i+1}^x + \sigma_i^y \sigma_{i+1}^y - \tfrac{1}{2}\sigma_i^z \sigma_{i+1}^z + \tfrac{1}{2} + \mathrm{i}\tfrac{\sqrt{3}}{2}\left(\sigma_i^z - \sigma_{i+1}^z\right)\right\} \tag{7}$$

and

$$e_0 = -\frac{1}{\sqrt{3}}\left(\frac{\mathrm{i}}{2}\sigma_1^z + \sigma_1^x - \frac{\sqrt{3}}{2}\right). \tag{8}$$

For our purposes, it becomes convenient to view the generators in terms of a tile in the bulk and a half-tile at the boundary.

$e_0 =$  $e_i =$ 

Products of generators at different sites, following the algebra relations, reduce to a subset of unique configurations. This is illustrated by the following two examples:

$e_4e_6e_1e_3e_5e_7 =$ 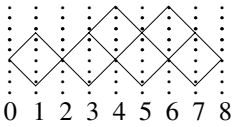

$e_0e_1e_3e_0e_2e_4e_6e_1e_3e_5e_7 =$ 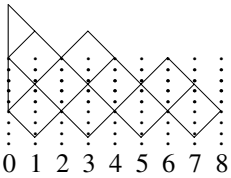

In terms of these generators, the stochastic Hamiltonians H for the RPMs can be written as

$$H^{(b)} = b(1 - e_0) + \sum_{i=1}^{L-1}(1 - e_i) \tag{9}$$

where b is the rate at the boundary and $u_d = u_a$ and we consider open boundary conditions only. In the following sections, we will consider the RPM with a rate at the boundary $b = 0$ and the RPMW with a rate $b = 1$. In the former case, a half-tile never attaches to the boundary, whereas in the latter, the half-tile may be attached to the boundary if it hits a positive slope. The following two examples illustrate the combinatorial properties for a small lattice with $L = 6$ in the RPM and for $L = 4$ in the RPMW.

$$H^{(0)} = \begin{pmatrix} -2 & 2 & 2 & 0 & 2 \\ 1 & -3 & 0 & 1 & 0 \\ 1 & 0 & -3 & 1 & 0 \\ 0 & 1 & 1 & -3 & 2 \\ 0 & 0 & 0 & 1 & -4 \end{pmatrix}$$

$$H^{(b)} = \begin{pmatrix} -3 & 0 & 0 & b & 0 & 0 \\ 1 & -2 & 1 & 0 & b & 0 \\ 1 & 1 & -2 & 1 & 0 & b \\ 1 & 0 & 1 & -2-b & 0 & 0 \\ 0 & 1 & 0 & 1 & -1-b & 2 \\ 0 & 0 & 0 & 0 & 1 & -2-b \end{pmatrix}$$

The ground-state eigenvectors of the intensity matrices (equation (9)) have remarkable combinatorial properties [4, 5, 10].

The wavefunctions $|0\rangle_L^{(b)}$ normalized to have the smallest entry equal to 1 (or b) are given by

$$|0\rangle_{L=6}^{(0)} = (11, 5, 5, 4, 1) \quad |0\rangle_{L=4}^{(b)} = (b^2, 3b(2+b), 2b(3+b), 3b, 3(2+b), 3). \tag{10}$$

Furthermore, the normalization expressions ${}^{(b)}\langle 0|0\rangle^{(b)}$ for $b = \{0, 1\}$ can be related to expressions describing alternating sign matrices [21]. This leads to known expressions for the normalization sequences for a given L as shown in table 1.

Table 1. Normalization expressions ${}^{(b)}\langle 0|0\rangle^{(b)}$ for even $L = (2n)$ for the RPM and the RPMW.

		L				
Model	Normalization	2	4	6	8	10
RPM ($b = 0$)	$A_V(2n+1)$	1	3	26	646	45 885
RPMW ($b = 1$)	$N_8(2n)A_V(2n+1)$	2	33	4420	4799 134	42 235 307 100

Here, $A_V(2n+1)$ is the number of vertically symmetric $(2n+1) \times (2n+1)$ alternating sign matrices [24–26]:

$$A_V(2n+1) = \prod_{j=0}^{n-1}(3j+2)\frac{(2j+1)!(6j+3)!}{(4j+2)!(4j+3)!} = 1, 3, 26, 646, 45\,885, \ldots \tag{11}$$

and $N_8(2n)$ is the number of cyclically symmetric transpose complement plane partitions [24, 21]:

$$N_8(2n) = \prod_{j=0}^{n-1}(3j+1)\frac{(2j)!(6j)!}{(4j)!(4j+1)!} = 1, 2, 11, 170, 7429, 920\,460, \ldots \tag{12}$$

The normalization sequences for the ground-state eigenvectors shown in table 1 will be related to probability expressions occurring in the RPM with a wall in section 5.

3. Energy spectra and spacetime phenomena

Throughout this paper, we assume $u \equiv u_a/u_d = 1$. In this case, the finite-sized corrections to the energy spectra of the intensity matrices $H^{(0)}$ and $H^{(1)}$ are given by a conformal field theory with the central charge ($c = 0$) [27–29]:

$$E_n = E_0 + \frac{\pi v(\Delta_s + n)}{L} + O(L^{-1}) \tag{13}$$

where n is an integer ($n \in \mathbb{N}$) labeling descendents and $v = \frac{3\sqrt{3}}{2}$ is the speed of sound in the system [5]. The conformal weights Δ_s are given by the following formula [27]:

$$\Delta_s = \frac{s(2s-1)}{3} = 0, 0, \frac{1}{3}, 1 \cdots \quad s = 0, \frac{1}{2}, 1, \frac{3}{2}, \cdots. \tag{14}$$

The Virasoro characters are given by (here, q is the modular parameter)

$$\chi_s(q) = q^{\Delta_s}(1 - q^{2s+1})\prod_{n=1}^{\infty}(1-q^n)^{-1}. \tag{15}$$

In table 2, the excited energy states E_n for different conformal weights (labeled by s) are compared to the numerical estimations obtained by diagonalizing the intensity matrices $H^{(0)}$ and $H^{(1)}$ (equation (9)) and extrapolating the results for $L \to \infty$.

Comparing both sides of table 2, we see that the energy levels of the RPM model coincide with the ones predicted by a conformal field theory with $\Delta_{s=0}$, while the RPMW model has different energy levels that can be explained by a conformal field theory with two conformal weights $\Delta_{s=0}$ and $\Delta_{s=\frac{1}{2}}$. Thus, there is an additional boundary operator in the model with a wall.

Next, we will turn to the time evolution of certain observables in the RPMW model. The expectation value of an observable X can be described using stochastic dynamics as

$$\langle X\rangle(t) = \langle 0|X\,\mathrm{e}^{-Ht}|\Psi(0)\rangle \tag{16}$$

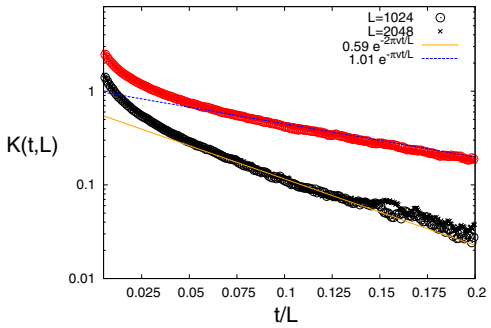

Figure 2. The time evolution of the average number of clusters $K(t)$ for RPM and RPMW. The lines represent the expected decay functions given by $K(t, L) \propto \mathrm{e}^{-E_1 t/L}$ with $E_1 = \frac{2v\pi}{L}$ (RPM) and $E_1 = \frac{v\pi}{L}$ (RPMW).

Table 2. Left: excited energy states $E_n \times L$ (in units of $v\pi$) for different values of s (equation (13)). Right: numerical approximations for $H^{(0)} \times L$ using up to $L = 18$ sites and for $H^{(1)} \times L$ using up to $L = 16$ sites.

		n					
s	Δ_s	0	1	2	3	4	5
$s = 0$	0	0	2	3	4	4	5
$s = \frac{1}{2}$	0	0	1	2	3	3	4
$s = 0 \bigoplus s = \frac{1}{2}$	0	0	1	2	2	3	3
		n					
Model	b	0	1	2	3	4	5
RPM	0	0.0000	2.0009	3.0035	4.0247	4.0257	5.037
RPMW	1	0.0000	1.0015	2.0087	1.9954	3.0030	3.0158

where the initial state $|\Psi(0)\rangle$ can be expanded in a complete eigenbasis characterizing the system $|\Psi(0)\rangle = \sum_n c_n |\psi_n\rangle$, and H is the stochastic matrix describing the system. Since H is an intensity matrix, the lowest eigenvalue is zero; hence, the lowest non-zero eigenvalue E_1 is expected to dominate the time evolution for large times. Let us consider the effect of adding a wall on temporal profiles of quantities describing the system. We are going to use Family–Vicsek [30] scaling in order to check if the system is in a scale-invariant phase (analogous to the RPM) and calculate the dynamical critical exponent z.

If we consider a time-dependent average quantity $x(t, L)$ with $x(L)$ being its average in the stationary state, we can define a function $X(t, L) = \frac{x(t,L)}{x(L)} - 1$ that scales for large t and L as

$$X(t, L) = \frac{x(t, L)}{x(L)} - 1 \sim X\left(\frac{t}{L^z}\right) \tag{17}$$

where z is the dynamical critical exponent.

We will apply this to a new quantity, the average number of clusters which we call $K(L)$ and which is defined as follows: a contact point is defined as a site i where $h_i = 0$ and a cluster is defined to be the domain between two contact points. Hence, the average number of clusters can be written as $K(L) = \langle \sum_i^L \delta_{h_i,0} \rangle$. This quantity is plotted in figure 2 as a function of time in the form given by equation (17). Thus, $X(t, L)$ becomes $K(t, L)$ here.

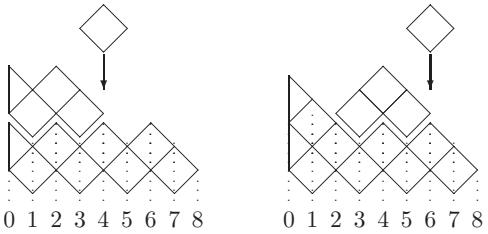

Figure 3. Examples of even and odd avalanches in RPMW. Avalanches occurring in the RPM release only an odd number of tiles.

The data collapse shows that the average number of clusters $K(t, L)$ has a critical exponent given by $z = 1$ for both RPM and RPMW. The long-time decay is described well by the exponential given by $E_1 = \frac{2\pi v}{L}$ for RPM and by $E_1 = \frac{\pi v}{L}$ for RPMW as expected from equation (16) for large times. This confirms that the time evolution of this stochastic system is described well by a conformal field theory expression in the presence of a wall.

4. Avalanches

Throughout this section, we always consider the boundary parameter $b = 1$. The RPM exhibits events where layers are evaporated from the substrate when a tile from the gas hits the interface. The number of tiles removed (v) defines the size of an avalanche. While this number is always an odd number in RPM, in RPWM, there is a possibility of an even number of tiles removed whenever an avalanche touches the boundary (the half-tile is counted as one tile). This is illustrated in figure 3.

It is known that the RPM with and without a wall exhibits self-organized criticality [6, 7] in the regime for $u \geqslant 1$ [4]. Desorption processes being non-local result in avalanches lacking a characteristic length scale. We denote by $S(v, L)$ the probability distribution function which gives the probability that an avalanche of size v occurs for a system of size L. This probability distribution $S(v, L)$ therefore appears as a power law which can be described in the finite-sized scaling (FSS) form [31, 3]

$$S(v, L) = v^{-\tau} F\left(\frac{v}{L^D}\right) \tag{18}$$

characterized by two exponents τ and D.

We would like to calculate these exponents for avalanches in which an odd, resp. even, number of tiles is removed. In order to obtain these exponents, the method of moments is used [4, 31]. Using the scaling form (equation (18)), we have

$$\langle v^m \rangle_L = \int S(v, L) v^m \, \mathrm{d}v = \int v^{-\tau} F\left(\frac{v}{L^D}\right) v^m \, \mathrm{d}v \tag{19}$$

$$= \int w^{-\tau} L^{-D\tau} F(w) w^m w^{mD} L^D \, \mathrm{d}w \tag{20}$$

$$= L^{D(1+m-\tau)} \underbrace{\int w^{m-\tau} F(w) \, \mathrm{d}w}_{\Gamma_m} = L^{\sigma(m)} \Gamma_m \tag{21}$$

Table 3. Estimates for the critical exponents in $S(v, L) \sim v^{-\tau} F(v/L^D)$ for even and odd avalanches using lattices $L = 4096$ and $L' = 8192$ for boundary parameter $b = 1$.

			$1/u$		
Exponent	Model	v	1.0	0.45	0.005
D	RPM [4]	Odd	1.004	1.026	1.006
	RPM [this work]	Odd	0.992 ± 0.058	1.015 ± 0.006	1.006 ± 0.0001
	RPMW [this work]	Odd	0.994 ± 0.025	1.008 ± 0.002	1.006 ± 0.0001
	RPMW [this work]	Even	0.980 ± 0.117	1.013 ± 0.008	1.006 ± 0.0001
τ	RPM [4]	Odd	3.000	2.25	2.00
	RPM [this work]	Odd	2.977 ± 0.079	2.224 ± 0.016	2.011 ± 0.001
	RPMW [this work]	Odd	3.003 ± 0.071	2.237 ± 0.012	2.011 ± 0.001
	RPMW [this work]	Even	1.932 ± 0.222	1.280 ± 0.074	1.020 ± 0.011

where we have used $w \equiv v/L^D$ to obtain the scaling dependence on L. We can obtain an estimate for the exponent $\sigma(m)$ by looking at the ratio:

$$\langle v^m \rangle_L / \langle v^m \rangle_{L'} = (L/L')^{\sigma(m)} \tag{22}$$

and in this manner, the exponent $\sigma(m)$ can be estimated as [1]

$$\sigma(m) = \frac{\ln(\langle v^m \rangle_L / \langle v^m \rangle_{L'})}{\ln(L/L')} = \begin{cases} 0 & \text{for} \quad m < \tau - 1 \\ D(1 + m - \tau) & \text{for} \quad m > \tau - 1. \end{cases} \tag{23}$$

A linear fit to equation (23) for $m > \tau - 1$ gives an estimate for the values of D and τ. To obtain an idea of the spread of these values, we ran several Monte Carlo simulations to find the variation of the distribution resulting from different seeds. The results are shown in table 3.

Results in this table show that the critical exponents for an *odd* number of tiles removed remain unchanged by adding a wall. However, we found that for an *even* number of tiles, the power-law exponent τ decreases by about 1.

We also found an interesting effect on the FSS function when the wall is added. Figure 4 shows the scaling function for RPM and RPMW for $u = 1$ and $1/u = 0.005$. In the first case, we use $\tau = 3.0$ and $\tau = 2.0$ for an *odd* number of tiles and an *even* number of tiles, respectively, while D is kept fixed at $D = 1$. The bottom part shows a similar plot where we use $\tau = 2.0$ and $\tau = 1.0$. The data collapse for large lattices shown in these plots confirms the FSS form (equation (4)). In these plots, we have rescaled $v \to (v + 1)/2$ for $v \in$ odd and $v \to v/2$ for $v \in$ even to compare the scaling function with the one given in [5].

This model can be compared to other models exhibiting self-organized criticality. There are different universality classes given by values of critical exponents observed in the respective models. The dynamics of the RPM is similar to the Manna model [32, 33], where the sites of a one-dimensional lattice are associated with integer values representing, e.g., particles or sand grains. If the particle occupation number is below a certain threshold, the respective site is considered to be inactive, whereas lattice sites with an occupation number larger than the threshold are active. The model evolves in time by the rules that all active sites redistribute their particles among randomly chosen nearest neighbors. However, comparing the critical exponents of the Manna model and the RPM, it is clear that the RPM and the RPMW are in a different universality class from the Manna model. In fact, the models discussed in this paper belong to a new universality class of non-equilibrium models as shown in [1–5]. Evidence for this fact provided in this paper includes the dynamical critical exponent $z = 1$ found at the Razumov–Stroganov point (the dynamical exponent for the Manna model being $z = 1.393(37)$ [33]) and the exponents D and τ calculated for the probability distribution function $S(v, L)$ (see table 3).

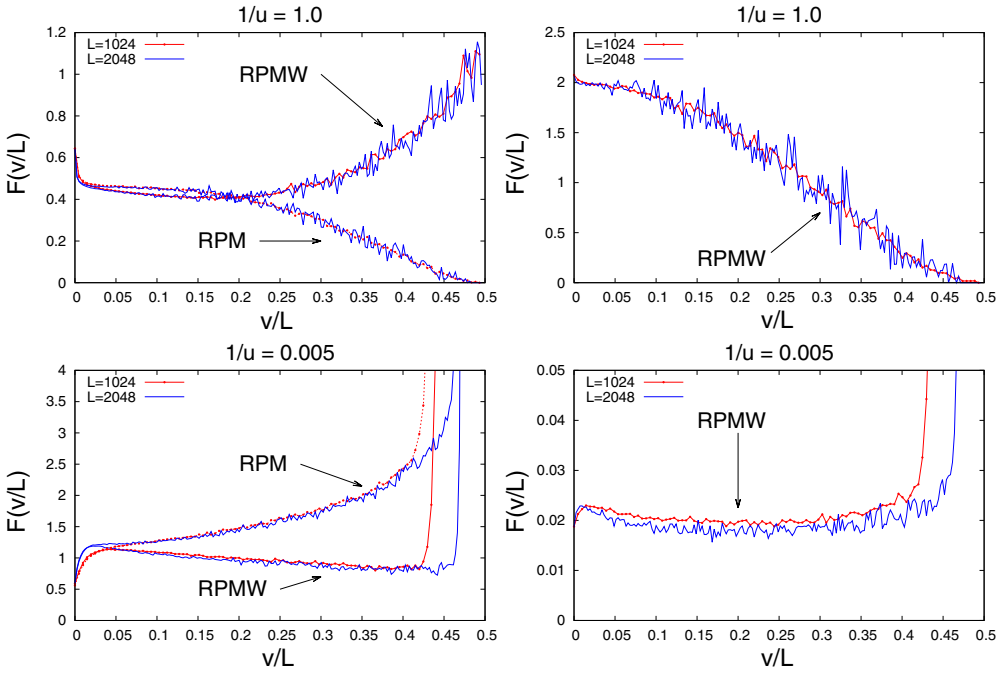

Figure 4. The scaling function $F(\frac{v}{L})$ versus v/L for different rates, $1/u = 1.0$ (top) and $1/u = 0.005$ (bottom). $b = 1$ for the RPMW. The left column shows the behavior for an *odd* number of tiles removed and the right column shows the behavior for an *even* number of tiles removed. The exponents used to show the data collapse are taken from table 3.

5. Conjectures for probabilities

In the RPM, three different processes may occur: absorption, desorption and reflection. Simple conjectures for the probabilities of these events have been established previously [1, 15]. In this section, we add some new conjectures for the RPMW. We will assume $u = 1$ and $b = 1$ for the RPMW throughout this paper.

The probability to lose (or gain) v tiles can be written by considering the rate of change between different states of the model:

$$P(v, L) = \sum_{\eta \neq \eta'} \delta(v(\eta') - v(\eta) - v) w_{\eta' \to \eta} P_{\eta'} / (\langle 0|0\rangle \times L). \tag{24}$$

Here, $w_{\eta' \to \eta}$ is the *transition rate* from state $|v(\eta')\rangle$ to state $|v(\eta)\rangle$, $P_{\eta'}$ denotes the frequency of the state $|v(\eta')\rangle$ occurring relative to other states, i.e. the coefficient in the right eigenvector given by equation (10), while the *denominator* corresponds to the sum of all possible transitions. With hindsight, the denominator can be written as $\langle 0|0\rangle \times L$ since there are known expressions for the normalization $\langle 0|0\rangle$ per unit length, at least for $u = 1$ (see table 1).

For certain cases, the expression above can be reduced to a nice ratio of algebraic expressions depending on the size of the system. Probabilities for the RPM were first reported in [1]. In this work, we focus on the RPMW. Table 4 shows the factorized numbers for the numerator and denominator for the RPMW for different cases obtained by diagonalizing the intensity matrices and obtaining the corresponding eigenvectors for values of L up to $L = 10$. This sequence can be used to conjecture expressions for the probabilities for the different

Table 4. Numerator and denominator terms for $P(v, L)$ (equation (24)) versus L for RPMW.

$P(v, L)$		L				
Numerator \ L		2	4	6	8	10
Absorption	$v = -1$	1	41	$2 \cdot 7 \cdot 17 \cdot 37$	$2^2 \cdot 17 \cdot 19 \cdot 23 \cdot 443$	$2 \cdot 3^4 \cdot 5^5 \cdot 19 \cdot 23^2 \cdot 29$
Reflection	$v = 0$	2	59	$2^2 \cdot 2819$	$2^3 \cdot 17 \cdot 19 \cdot 6143$	$2 \cdot 3 \cdot 5 \cdot 13 \cdot 19 \cdot 23^2 \cdot 43759$
Desorption	$v > 0$	1	$2 \cdot 3^2 \cdot 5$	$2 \cdot 3 \cdot 29 \cdot 37$	$2^2 \cdot 13 \cdot 17 \cdot 19 \cdot 557$	$2^2 \cdot 3 \cdot 5 \cdot 19 \cdot 23^2 \cdot 83 \cdot 2063$
	Even	0	1	$2^3 \cdot 3^3$	$2^3 \cdot 17 \cdot 19 \cdot 113$	$2 \cdot 3 \cdot 5 \cdot 19 \cdot 23^3 \cdot 421$
	Odd	1	31	$2 \cdot 3 \cdot 17 \cdot 61$	$2^2 \cdot 5 \cdot 17 \cdot 19 \cdot 23 \cdot 61$	$2 \cdot 3^4 \cdot 5^3 \cdot 17 \cdot 19 \cdot 23^2 \cdot 29$
Parity	Odd	2	$2^3 \cdot 3^2$	$2^2 \cdot 13 \cdot 17^2$	$2^4 \cdot 11 \cdot 17^2 \cdot 19 \cdot 23$	$2^2 \cdot 3^5 \cdot 5^3 \cdot 7 \cdot 19 \cdot 23^2 \cdot 29$
	Even	2	$2^2 \cdot 3 \cdot 5$	$2^2 \cdot 13^2 \cdot 17$	$2^7 \cdot 17^2 \cdot 19 \cdot 23$	$2^2 \cdot 3^2 \cdot 5^3 \cdot 7 \cdot 19^2 \cdot 23^2 \cdot 29$
Denominator \ L		2	4	6	8	10
$^{(1)}\langle 0\|0\rangle^{(1)} \cdot L$		2^2	$2^2 \cdot 3 \cdot 11$	$2^3 \cdot 3 \cdot 5 \cdot 13 \cdot 17$	$2^4 \cdot 17^2 \cdot 19^2 \cdot 23$	$2^3 \cdot 3^2 \cdot 5^3 \cdot 7 \cdot 19 \cdot 23^3 \cdot 29$

Table 5. Conjectured probabilities for absorption $P_a \equiv P(-1, L)$, desorption $P_d \equiv P(v > 0, L)$ and reflection $P_r \equiv P(0, L)$. These conjectures have been checked with exact diagonalization up to $L = 10$. In the last row, we show results obtained with MC using lattices up to $L = 2048$ for the individual probabilities P_d and P_r for $v \in$ even.

$P(v, L)$	v	P_a	P_d	P_r	$P_a + P_d + P_r$
RPM	Odd	$\frac{3L(L-2)}{4(2L+1)(L-1)}$	$\frac{2(L-2)(L+2)}{4(2L+1)(L-1)}$	–	$\frac{5L^2-6L-8}{4(2L+1)(L-1)}$
	0	–	–	$\frac{3L^2+2L+4}{4(2L+1)(L-1)}$	$\frac{3L^2+2L+4}{4(2L+1)(L-1)}$
RPMW	Odd	$\frac{6L^2+8L-5}{4(2L+1)(2L+3)}$	$\frac{4L^2+5L+9}{4(2L+1)(2L+3)}$	–	$\frac{10L^2+13L+4}{4(2L+1)(2L+3)}$
	Even/0	–	$\frac{1.8L-4.9}{4(2L+1)(2L+3)}$	$\frac{6L^2+17.2L+12.7}{4(2L+1)(2L+3)}$	$\frac{6L^2+19L+8}{4(2L+1)(2L+3)}$

cases for arbitrary L. In this table, we denote the case of absorption by $v = -1$, the case of reflection by $v = 0$ and the case of desorption of v tiles by $v > 0$.

Table 5 shows the probabilities for avalanches with even or odd numbers of tiles removed for a given L for both RPM and RPMW. Expressions for $P(v, L)$ for RPM were first written by de Gier *et al* [1], and recently Alcaraz *et al* [15] provided the probability of absorption (P_a) for RPMW.

In this work, we show that by splitting the desorption probability (P_d) into its even and odd components, we obtain a nice expression for the desorption case when an odd number of tiles is removed. However, for the even case, a simple factorization for the reflection and desorption probability is not apparent. The coefficients remain non-integer numbers within the precision of our fits. Only the sum $P_a + P_d + P_r$ has an expression with integer coefficients. The error bars on the fits leading to non-integer coefficients are as follows:

$$P_d(\text{even}) = \frac{(1.805 \pm 0.002)L + (-4.77 \pm 0.04)}{4(2L+1)(2L+3)}$$

$$P_r = \frac{(5.999\,95 \pm 0.000\,04)L^2 + (17.201 \pm 0.003)L + (12.66 \pm 0.04)}{(4(2L+1)(2L+3)}.$$

We also tried to obtain fits assuming higher order polynomials for the denominators (e.g. quartic polynomials), but the errors were even bigger. The culprit is probably the probability of desorption for an even number of tiles removed, as can be seen from the following argument.

This probability is the only one vanishing algebraically as $P_d(v \text{ even}) \sim L^{-1}$ in the large-L limit, whereas all other probabilities given in the table become finite expressions as $L \to \infty$. This is consistent with the scaling exponent for avalanche distributions with an even number

of tiles removed differing by 1 from the exponent for avalanches with an odd number of tiles removed. The reason for avalanches with an even number of tiles removed vanishing in the large-L limit has to do with the fact that these avalanches always touch the boundary. Hence, they become more rare as the size of the system increases.

There is an alternative approach that allows us to quantify the accuracy of the numerical results. The mean size of an avalanche $\langle v\rangle$ in the stationary state can be obtained from the following mean-field expression taken from [4]:

$$\langle v\rangle_L = P_a(L)/P_d(L). \tag{25}$$

This is a quotient of parabolas, and in the large limit ($L \gg 1$),

$$\begin{aligned}\frac{P_a(L)}{P_d(L)} &= \frac{\alpha L^2+\beta L+\gamma}{aL^2+bL+c}\\ &= \frac{\alpha L^2+\beta L+\gamma}{aL^2\left(1+\frac{b}{aL}+\frac{c}{aL^2}\right)}\\ &\approx \left(\frac{\alpha}{a}+\frac{\beta}{aL}+\mathcal{O}(L^{-2})\right)\left(1-\frac{b}{aL}+\mathcal{O}(L^{-2})\right)\\ &\approx \left(\frac{\alpha}{a}+\frac{\beta}{aL}-\frac{\alpha b}{a^2L}+\mathcal{O}(L^{-2})\right)\\ &= \left(\frac{\alpha}{a}+\frac{1}{aL}\left(\beta-\frac{\alpha b}{a}\right)\right)\\ &= \frac{\alpha}{a}\left(1+\frac{1}{L}\left(\frac{\beta}{\alpha}-\frac{b}{a}\right)\right).\end{aligned} \tag{26}$$

We assume that $\alpha \neq 0$ and $a \neq 0$ and dropped terms of the order of $\mathcal{O}(L^{-2})$). In the following, we consider v to be odd only. From table 5, we see that for RPM, we have in that case

$$\begin{aligned}\frac{P_a(L)}{P_d(L)} &= \frac{3}{2}\left(1-\frac{1}{L}\left(\frac{6}{3}-\frac{0}{2}\right)\right)\\ \Rightarrow \langle v\rangle_L &= \frac{3}{2}\left(1-\frac{2}{L}\right)\end{aligned} \tag{27}$$

while for RPMW, we have

$$\begin{aligned}\frac{P_a(L)}{P_d(L)} &= \frac{6}{4}\left(1+\frac{1}{L}\left(\frac{8}{6}-\frac{6.8}{4}\right)\right)\\ \Rightarrow \langle v\rangle_L &= \frac{3}{2}\left(1-\frac{0.366}{L}\right).\end{aligned} \tag{28}$$

The average avalanche size $\langle v\rangle(L)$ obtained from Monte Carlo simulations of the RPM and the RPMW agrees quite well with these predictions as can be seen in figure 5. This is remarkable since this describes a non-equilibrium system.

It is interesting to see that the leading term in this expansion is universal, whereas the correction term depends on the details of the model (i.e. whether there is a wall or not). This is similar behavior as in FSS of the concentration of particles in certain reaction–diffusion systems [34–36] and surface exponent corrections to quantum chains using different types of boundary conditions [37–39].

The simple functional form for the probabilities shown in table 5 suggests that we can guess a general quadratic expression in L for the probabilities $P(v, L)$ by fixing the denominator as

$$P_{\mathrm{RPM}}(v, L) = \frac{a(v)L^2+b(v)L+c(v)}{4(2L+1)(L-1)} \tag{29}$$

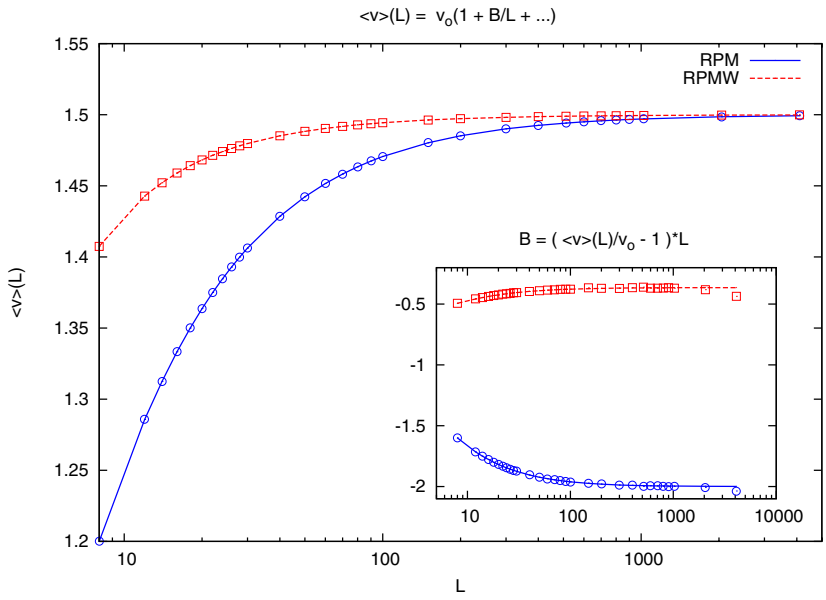

Figure 5. Average avalanche size $\langle v \rangle(L)$. Predictions from the ratio of $P_a(L)/P_d(L)$ given by equations (27) and (28), respectively (lines) compared to Monte Carlo data for RPM (◯) and RPMW (□). The inset figure shows the correction terms calculated from equations (27) and (28).

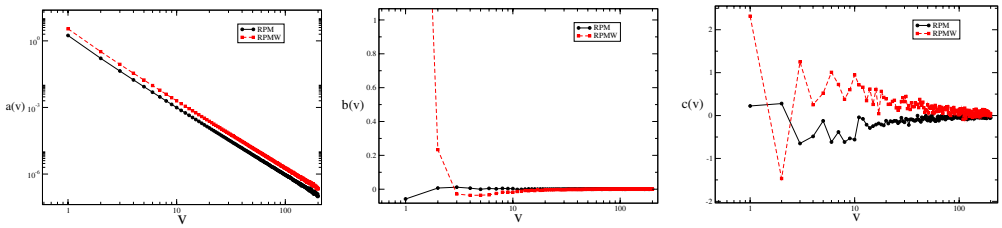

Figure 6. Behavior of the quadratic term $a(v)$, linear term $b(v)$ and constant term $c(v)$ obtained from fits to equations (29) and (30).

$$P_{\mathrm{RPMW}}(v, L) = \frac{a(v)L^2 + b(v)L + c(v)}{4(2L+3)(2L+1)} \tag{30}$$

and fitting for the parameters $\{a(v),\ b(v),\ c(v)\}$ in the forms (29) and (30). The behavior of these parameters as a function of v is shown in figure 6. As expected, the quadratic term shows power-law behavior $\propto v^{-3.0}$. The linear and constant terms however do show different behavior, but we were not able to reduce it to an analytical form. Consistency of the fits demands that (see table 5)

$$\sum_{v>0} P_{\mathrm{RPM}}(v, L) = \frac{2L^2 - 8}{4(2L+1)(L-1)} \tag{31}$$

$$\sum_{v>0} P_{\mathrm{RPMW}}(v, L) = \frac{4L^2 + 5L + 9}{4(2L+3)(2L+1)}. \tag{32}$$

Table 6. Sums over v for the parameters $a(v)$, $b(v)$ and $c(v)$ resulting from the fits.

	$\sum_v a(v)$	$\sum_v b(v)$	$\sum_v c(v)$
RPM	1.999 99	−0.003 75	−13.8002
RPMW	3.999 97	4.966 04	30.4445

The sums over the parameters $\sum_v \{a(v), b(v), c(v)\}$ are shown in table 6 for RPM and RPMW. We see that the quadratic $a(v)$ and linear $b(v)$ terms capture the behavior in v quite well, whereas as shown in figure 6, the constant term $c(v)$ is dominated by the fluctuations.

6. Conclusion

We studied the non-equilibrium statistical model known as the raise and peel model (RPM). We have confirmed that this model retains several features as predicted from conformal invariance when the boundary conditions are changed. We allowed one boundary to fluctuate and demonstrated that the temporal profile of a stochastic quantity follows its expected behavior from stochastic dynamics where the long-time behavior is dominated by the lowest non-zero eigenvalue. We studied the surface dynamics by looking at avalanche distributions exhibiting power-law distributions. Using the finite-sized scaling formalism, we confirmed the universality exponent $\tau = 3$ for the RPM with different boundary conditions and identified an even/odd effect with a new exponent $\tau = 2$ for avalanches with an even number of tiles removed. We also found new conjectures for the probability of desorption and reflection with a wall added to the system and checked that they agree with Monte Carlo data.

In the context of surface critical phenomena, it is interesting to ask how the presence of the wall in the RPMW changes its phase diagram. For the case without a wall, the full phase diagram is given in [5]. It depends only on the parameter u and consists of a massive phase for $0 \leqslant u < 1$ and a scale-invariant phase for $1 < u < \infty$. At $u = 1$, the model is massless and conformal-invariant. This work shows that in the presence of a wall, the integrable point remains at $u = 1$ where the model is still given by a conformal field theory with $c = 0$; the conformal field theory has an additional boundary operator compared to the conformal field theory for the RPM. Furthermore, there is a phase exhibiting self-organized criticality for $u \leqslant 1$; in comparison with the RPM, there are new critical exponents in the SOC phase which occur for an even number of tiles removed in an avalanche as explained above. The detailed exploration of the full phase diagram for the RPMW is left for a future publication.

Acknowledgments

We would like to thank V Rittenberg for valuable discussions over the years which originally sparked this work. We also would like to thank M Henkel and the Groupe de Physique Statistique at Nancy University for helpful discussions. BW-K gratefully acknowledges support from the NSF under the grant PHY-0969689.

References

[1] Pearce P A, de Gier J, Nienhuis B and Rittenberg V 2003 Stochastic processes and conformal invariance *Phys. Rev.* E **67** 016101

[2] Pearce P A, de Gier J, Nienhuis B and Rittenberg V 2004 The raise and peel model of a fluctuating interface *J. Stat. Phys.* **114** 1–35

[3] Alcaraz F C, Droz M, Henkel M and Rittenberg V 1994 Reaction–diffusion processes, critical dynamics, and quantum chains *Ann. Phys.* **230** 250–302

[4] Alcaraz F C, Levine E and Rittenberg V 2006 Conformal invariance and its breaking in a stochastic model of a fluctuating interface *J. Stat. Mech.* **2006** P08003

[5] Alcaraz F C and Rittenberg V 2007 Different facets of the raise and peel model *J. Stat. Mech.* **2007** P07009

[6] Bak P, Tang C and Wiesenfeld K 1988 Self-organized criticality *Phys. Rev.* A **38** 364–74

[7] Dhar D 1999 Studying self-organized criticality with exactly solved models arXiv:cond-mat/9909009

[8] Razumov A V and Stroganov Y G 2001 Spin chains and combinatorics *J. Phys. A: Math. Gen.* **34** 3185

[9] Razumov A V and Stroganov Y G 2001 Spin chains and combinatorics: twisted boundary conditions *J. Phys. A: Math. Gen.* **34** 5335

[10] de Gier J 2007 The Razumov–Stroganov conjecture: stochastic processes, loops and combinatorics *J. Stat. Mech.* **2007** N02001

[11] de Gier J, Batchelor M T and Nienhuis B 2001 The quantum symmetric XXZ chain at $\delta = \frac{-1}{2}$, alternating-sign matrices and plane partitions *J. Phys. A: Math. Gen.* **34** L265

[12] Alcaraz F C and Martins M J 1989 Conformal invariance and the operator content of the XXZ model with arbitrary spin *J. Phys. A: Math. Gen.* **22** 1829

[13] van Beijeren H (ed) 1990 *Fundamental Problems in Statistical Mechanics VII: Proc. 7th Int. Summer School on Fundamental Problems in Statistical Mechanics (Altenburg, Germany, 18–30 June 1989)* (Amsterdam: North-Holland)

[14] Henkel M 1999 *Conformal Invariance and Critical Phenomena* (Berlin: Springer)

[15] Alcaraz F C, Pyatov P and Rittenberg V 2008 Density profiles in the raise and peel model with and without a wall, physics and combinatorics *J. Stat. Mech.* **2008** P01006

[16] Pyatov P 2004 Raise and peel models of fluctuating interfaces and combinatorics of Pascal's hexagon *J. Stat. Mech.* **2004** P09003

[17] Alcaraz F C and Rittenberg V 1993 Reaction–diffusion processes as physical realizations of Hecke algebras *Phys. Lett.* B **314** 377–80

[18] Golinelli O and Mallick K 2006 The asymmetric simple exclusion process: an integrable model for non-equilibrium statistical mechanics *J. Phys. A: Math. Gen.* **39** 12679

[19] de Gier J, Pearce P A, Rittenberg V and Nienhuis B 2002 Temperley–Lieb stochastic processes *J. Phys. A: Math. Gen.* **35** L661

[20] Nichols A, Rittenberg V and de Gier J 2005 One-boundary Temperley–Lieb algebras in the XXZ and loop models *J. Stat. Mech.* **2005** P03003

[21] de Gier J and Rittenberg V 2004 Refined Razumov–Stroganov conjectures for open boundaries *J. Stat. Mech.* **2004** P09009

[22] Martin P and Saleur H 1994 The Blob algebra and the periodic Temperley–Lieb algebra *Lett. Math. Phys.* **30** 189

[23] Martin P and Woodcock D 2000 On the structure of the Blob algebra *J. Algebra* **225** 957

[24] Mitra S, Nienhuis B, de Gier J and Batchelor M T 2004 Exact expressions for correlations in the ground state of the dense O(1) loop model *J. Stat. Mech.* **2004** P09010

[25] de Gier J 2005 Loops, matchings and alternating-sign matrices *Discrete Math.* **298** 365–88

[26] Propp J 2001 The many faces of alternating-sign matrices *Discrete Mathematics and Theoretical Computer Science Proc. AA (DM-CCG)* pp 43–58

[27] Pearce P A, Rittenberg V and de Gier J 2001 Critical $q = 1$ Potts model and Temperley–Lieb stochastic processes arXiv:cond-mat/0108051

[28] de Gier J, Nichols A, Pyatov P and Rittenberg V 2005 Magic in the spectra of the XXZ quantum chain with boundaries at and *Nucl. Phys.* B **729** 387–418

[29] Yang X and Fendley P 2004 Non-local spacetime supersymmetry on the lattice *J. Phys. A: Math. Gen.* **37** 8937

[30] Family F and Vicsek T 1985 Scaling of the active zone in the eden process on percolation networks and the ballistic deposition model *J. Phys. A: Math. Gen.* **18** L75

[31] Tebaldi C, De Menech M and Stella A L 1999 Multifractal scaling in the Bak–Tang–Wiesenfeld sandpile and edge events *Phys. Rev. Lett.* **83** 3952–5

[32] Manna S S 1991 Two-state model of self-organized criticality *J. Phys. A: Math. Gen.* **24** L363–9

[33] Hinrichsen H, Henkel M and Lübeck S 2008 *Non-Equilibrium Phase Transitions: Absorbing Phase Transitions* vol 1 (Berlin: Springer)

[34] Krebs K, Pfannmüller M, Wehefritz B and Hinrichsen H 1995 Finite-size scaling studies of one-dimensional reaction–diffusion systems: part I. Analytical results *J. Stat. Phys.* **78** 1429–70

[35] Krebs K, Pfannmüller M, Simon H and Wehefritz B 1995 Finite-size scaling studies of one-dimensional reaction–diffusion systems: part II. Numerical methods *J. Stat. Phys.* **78** 1471–91

[36] Bilstein U and Wehefritz B 1999 The XX-model with boundaries: part I. Diagonalization of the finite chain *J. Phys. A: Math. Gen.* **32** 191

[37] Alcaraz F C, Barber M N, Batchelor M T, Baxter R J and Quispel G R W 1987 Surface exponents of the quantum XXZ, Ashkin–Teller and Potts models *J. Phys. A: Math. Gen.* **20** 6397
[38] Turban L and Igli F 1997 Off-diagonal density profiles and conformal invariance *J. Phys. A: Math. Gen.* **30** L105
[39] Burkhardt T W and Xue T 1991 Density profiles in confined critical systems and conformal invariance *Phys. Rev. Lett.* **66** 895–8